

Soft inclusion in a confined fluctuating active fluid

Amit Singh,¹ J. F. Rupprecht,² G.V. Shivashankar,² J. Prost,^{2,3} and Madan Rao¹

¹*Simons Centre for the Study of Living Machines, National Centre for Biological Sciences (TIFR), Bangalore 560065, India*

²*Mechanobiology Institute and Department of Biological Sciences, National University of Singapore, Singapore*

³*Sorbonne Universities, UPMC Univ Paris 06, CNRS, Laboratoire Physico Chimie Curie, Paris (France).*

(Dated:)

We study stochastic dynamics of an inclusion within a one dimensional confined viscous active fluid. To highlight various features and to appeal to different contexts, the inclusion is in turn treated as a rigid element, an elastic element and a viscoelastic (Kelvin-Voigt) element. We show that the dynamics for the shape and position of the inclusion can be described by coupled Langevin equations with a confining potential and multiplicative noise. Deriving exact expressions for the corresponding steady state probability distributions, we find that the active noise induces an attraction to the edges of the confining domain. In the presence of a competing centering force, we find that the shape of the probability distribution exhibits a sharp transition upon varying the amplitude of the active noise. Our results could help understanding the positioning and deformability of biological inclusions, eg. organelles in cells, or nucleus and cells within tissues.

I. INTRODUCTION

The collective fluctuating dynamics of particles in a medium, each of which are driven out of equilibrium by dissipation of energy, is a fundamentally new branch of statistical physics [1], with deep implications for the physics of cells and tissues [1, 2]. More recent studies have focussed on the effects of confinement on active matter, especially on the nature of forces on fixed or deformable boundaries, as a result of specific boundary conditions [3]. However, the role of fluctuations in generating novel forces at the boundaries of confined active suspensions, have not received adequate attention. Such studies have potential implications for the fluctuating dynamics of organelles embedded within the cell cytoplasm, described as an active actomyosin suspension.

In this paper, we study the positioning and shape dynamics of a deformable inclusion embedded in a confined active fluid. Formulated in this general way, our study is applicable to a variety of in-vivo and in-vitro contexts - (i) the positioning and shape fluctuations of the nucleus (or other localized organelles) within a cell [4–8], (ii) the dynamics of large colloidal particles embedded in an active medium [9–12], (iii) the positioning and dynamics of nuclei in multi-nucleated cells [13], (iv) the positioning and segregation of chromosomes within a nucleus [14–17] and (v) the fluctuations of a cell / cell-junction within a developing tissue [18, 19].

For concreteness, we consider that the inclusion represents the cell nucleus that is connected to the cell cortex, whose boundary is held fixed, for instance by surface attachment on a micro-patterned substrate coated with fibronectin [7, 20, 21] (Fig. 1(a)).

At a conceptual level and to make general comparisons with experiments such as [7], it suffices to study the problem in 1 dimension (1d). We start by setting up the general equations valid for any type of inclusion in Section II. To highlight different aspects we in turn treat the inclusion as being a rigid element (Section III), an elastic element (Section IV) and a viscoelastic (Kelvin-

Voigt) element (Section V), each embedded in an active fluid.

We find that in general, the active dynamics of the position and shape of the inclusion are described by coupled Langevin equations with a confining potential and *multiplicative* noise. Solving the Fokker-Planck equations corresponding to the Langevin description, we obtain the exact steady state distributions for the position and size of the inclusion.

Our analysis shows that there are *sharp transitions* in the nature of the probability distribution, as a function of the relative strength of the confining potential and active noise. The cell boundary influences the steady state position, and size of the inclusion. The position, and size fluctuations of the inclusion are also driven by these active stress fluctuations in the active fluid.

This paper follows the Letter [21] which contains a comparison to experiments on the positioning and fluctuations of the nucleus in cells confined in micropatterned surfaces.

The dynamics of the inclusion embedded in the fluctuating active fluid can be viewed as an active Casimir effect [22–24]. We show that this fluctuation-induced attraction depends on both the intensity of the active noise and on the hydrodynamic interactions of the inclusion with the boundaries. We find that the effect of such Casimir-type forces on the boundary confining a dilute active suspension, extends over large scales (Section VI).

II. BASIC EQUATIONS

For the purposes of this presentation, we treat the active gel surrounding the inclusion and confined by the cell boundary as an active Stokes fluid (Fig. 1(a)); we are thus interested in the dynamics at time scales larger than the Maxwell stress relaxation time [25] and the time scale over which inertia of the inclusion gets damped. The active Stokesian fluid comprises a collection of stochastic force dipoles - characterising the statistics of remodelling

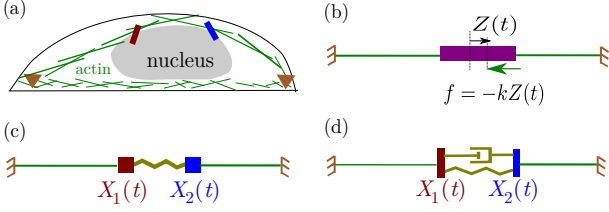


FIG. 1. (a) Schematic of the cell nucleus embedded in an active cytoplasm and confined by actin stress fibres. Following [21], we model the nucleus as an inclusion embedded in an active fluid confined by the cell boundary. To address various possible contexts, we treat the inclusion in turn as (b) a passive rigid element (Sec. III), (c) an elastic element (Sec. IV) and (d) a viscoelastic (Kelvin-Voigt) element (Sec. V).

of actomyosin - represented by an active noise that is correlated over a finite time. In our treatment, we study the stochastic dynamics over time scales larger than the active stress correlation time τ . For the specific case of the dynamics of the nuclear inclusion in the cell cytoplasm, see [21]. In the following, we proceed with a one-dimensional (1d) realization.

We consider an inclusion (I) embedded in a 1d active fluid confined between hard walls at $x = \pm L$ (Fig. 1(b)-(d)). We denote the edges of the inclusion as $x_1(t) \leq x_2(t)$ and the viscous fluid regions to the left and right of the inclusion as (L) and (R), respectively.

The hydrodynamic variables describing the bulk are the actomyosin concentration c and the hydrodynamic velocity v . The velocity field of this active Stokesian fluid is determined by local force balance, $\partial_x \sigma(x, t) = 0$. We express the local stress as

$$\sigma^{L,R} = \eta_c \partial_x v - \zeta \Delta \mu c + \vartheta, \quad (1)$$

where η_c is a one-dimensional cortical viscosity, $\zeta \Delta \mu < 0$ is the active contractile stress [1, 2, 26]. Here, ϑ represent stress fluctuations which may either be of thermal or active origin. Under the assumption of a constant viscosity η_c , the fluctuation-dissipation relation imposes thermal fluctuations should be delta-correlated: $\langle \vartheta(x, t) \vartheta(x', t') \rangle = 2\Lambda_c \delta(x - x') \delta(t - t')$. In contrast, we assume that active fluctuations are an exponentially correlated process

$$\langle \vartheta(x, t) \vartheta(x', t') \rangle = 2\Lambda_c \frac{e^{-|t-t'|/\tau}}{\tau} \delta(x - x'). \quad (2)$$

Such a finite correlation time τ in the noise is incompatible with the fluctuation-dissipation relation blue(FDR)[27].

Since we are interested in the dynamics over time scales larger than the noise correlation time τ , we consider that the short correlation time limit $\lim_{\tau \rightarrow 0} \tau^{-1} \exp(-|t - t'|/\tau) = \delta(t - t')$, in which ϑ becomes a Gaussian white noise with $\langle \vartheta \rangle = 0$ and $\langle \vartheta(x, t) \vartheta(x', t') \rangle = 2\Lambda_c \delta(x - x') \delta(t - t')$. In principle, there is also a contribution from thermal fluctuations which we take to be small com-

pared to active fluctuations. In Appendix A, we detail the method to obtain the proper thermal limit.

The inclusion will be treated in turn as a passive rigid element, a passive elastic element and a viscoelastic (Kelvin-Voigt) element. We denote the bulk stress in the inclusion as $\sigma^I(t)$, whose form we discuss in subsequent sections. In general, there could also be a stress at the boundary between the inclusion and the embedding active fluid, arising for instance from a confining force, $f(x)$, which favours a centering of the nucleus. This could arise from a variety of sources, such as confinement due to microtubules and motors [4–6], or the geometry of stress fibres constraining the nucleus [21, 28].

We now specify the boundary conditions both at the edges of the inclusion and the rigid confining walls. We choose velocity continuity at the boundaries of the inclusion $v^I(x_1) = v^L(x_1)$ and $v^I(x_2) = v^R(x_2)$, and either *no flow* $v(-L) = v(L) = 0$ or *finite flow* $v(-L) = v_L, v(L) = -v_R$, at the confining walls.

The local force balance $\partial_x \sigma = 0$ implies that the stress is constant $\sigma = \sigma(t)$ within each left and right segments. Integrating Eq. 1 over x in the regions (L) and (R), we obtain that

$$\eta_c \dot{x}_1 = \eta_c v_L + (x_1 + L) \sigma^L(t) + \zeta \Delta \mu c_L - \int_{-L}^{x_1} \vartheta dx \quad (3)$$

$$\eta_c \dot{x}_2 = -\eta_c v_R + (x_2 - L) \sigma^R(t) - \zeta \Delta \mu c_R + \int_{x_2}^L \vartheta dx, \quad (4)$$

where $c_L = \int_{-L}^{x_1} c(x) dx$ and $c_R = \int_{x_2}^L c(x) dx$ are the total bulk concentrations of actomyosin. We analyse the limit when the turnover of actomyosin is fast, this gives rise to a constant *local actomyosin density* c_0 , thus, $c_L = (x_1 + L)c_0$ and $c_R = (L - x_2)c_0$. In Appendix B, we discuss the limit of slow actomyosin turnover, when the *total actomyosin number* c_L, c_R can be taken to be constant. In the fast turnover limit, Eqs. 3 and 4 become to

$$\eta_c \dot{x}_1 = (x_1 + L)(\sigma^L(t) + \zeta \Delta \mu c_0) + \eta_c v_L - \sqrt{x_1 + L} \theta_1, \quad (5)$$

$$\eta_c \dot{x}_2 = (x_2 - L)(\sigma^R(t) + \zeta \Delta \mu c_0) - \eta_c v_R + \sqrt{L - x_2} \theta_2, \quad (6)$$

where θ_1 and θ_2 are Gaussian white noise of variance $2\Lambda_c$ which originates from the spatial integration of the fluctuating stress: $\int_a^b \vartheta_A dx = \sqrt{b - a} \theta_A(t)$.

We point out that Eqs. 5-6 relate the coordinates of the inclusion edges x_1 and x_2 to the bulk stresses σ^L and σ^R . These bulk stresses are determined by the bulk flows generated by the active stress and the stress in the inclusion (I). These are related by stress continuity, $\partial_x \sigma(x, t) = 0$: $[\sigma^L(t) - \sigma^I(t)] = f(x_1)$ and $[\sigma^R(t) - \sigma^I(t)] = -f(x_2)$, where f is the confining force acting on the boundaries of the inclusion.

We thus see that the confinement gives rise to a multiplicative noise on the dynamics of the inclusion. This

arises from an interplay between hydrodynamic interaction, confinement and fluctuations.

As in any situation with multiplicative noise, we must provide an interpretation of the noise term in order to give meaning to Eqs. 5-6 [29, 30]. The noises θ_1, θ_2 are active, violate FDR, and are the large time limit of an exponentially correlated process [27]. As discussed in [29–31] (see Appendix A), when the inertial relaxation time is much smaller than the noise correlation time, as is appropriate for our treatment, the Langevin Eqs. 5-6 should be analyzed by the *Stratonovich* [29, 32] convention.

However, we would also like our equations to describe situations when the noise is thermal and FDR holds. In this case, the noise correlation time is much smaller than the inertial relaxation time, and we must interpret Eqs. 5-6 in the *Hanggi-Klimontovich* [33, 34] convention, which recovers FDR and Boltzmann distribution at steady state [35, 36]. In the final analysis, there ought to be absolutely no ambiguity if one includes in the stochastic dynamics, the correct dynamics of the concentration c , which is the physical source of the noise.

TABLE I. List of notations

α	Convention on the Langevin equations
$2\Lambda_c$	Variance of the noise
η_c	Viscosity of the gel
η_I	Viscosity of the inclusion
$f(z)$	Force on the inclusion
$\Delta\mu c$	Active stress term
v_L	Gel velocity on the left boundary
v_0	Velocity in the case: $v_L = -v_R = v_0$
c_0	Local density of contractile elements
c_L	Integrated density on the left
l	Preferred half-length of the inclusion
k	Strength of an harmonic confinement
$r = \eta_c/\eta_I$	Inclusion to Bulk viscosity ratio
ϵ	Width of the boundary regions
B	Elastic modulus of inclusion
$b = (B\eta_c 2l)/\Lambda_c$	Normalized elastic modulus
$\tilde{L} = L - l$	Half-length of the gel in Sec. III
$y = x_2 - x_1$	Length of the inclusion
$z = x_2 + x_1$	Center of mass position

III. RIGID INCLUSION IN AN ACTIVE FLUID

We first model the inclusion as a rigid object of fixed size $x_2 - x_1 = 2l$; being rigid, the confining force applied at the boundary of the inclusion can be transferred to the centre-of-mass (COM) coordinate $z \equiv (x_1 + x_2)/2$ (see also Fig. 1(b)). Now the stresses are related by $\sigma^L(t) = \sigma^R(t) + f(z)$.

Combining Eqs. 5 and 6, we find that the dynamics of the COM coordinate reads

$$\dot{z} = -\frac{v_0}{2\tilde{L}}z + f(z)\frac{(\tilde{L}^2 - z^2)}{2\eta_c\tilde{L}} + \sqrt{\frac{\Lambda_c}{\eta_c^2}\frac{(\tilde{L}^2 - z^2)}{\tilde{L}}}\theta, \quad (7)$$

where we define the length $\tilde{L} = L - l$, the velocity $v_L = -v_R = v_0$ and the Gaussian white noise of unit variance θ .

As noted above, this Langevin dynamics with multiplicative noise arises as an interplay between hydrodynamic interaction, confinement and fluctuations.

The $\tilde{L}^2 - z^2$ term above is a consequence of the long range hydrodynamic interaction between the confining wall and the inclusion, which allows the effect of the boundary to be felt far into the bulk.

The Langevin equation, for both thermal and active cases, is of the general form, $\dot{x} = F(x) + G(x)\theta(t)$, for which the corresponding Fokker-Planck equation is [35],

$$\partial_t P = \partial_x \left(-F(x) - \alpha G(x)G'(x) + \frac{1}{2}\partial_x G^2(x) \right) P$$

where $\alpha = 1$ (Hanggi-Klimontovich) corresponds to the thermal case and $\alpha = 1/2$ (Stratonovich) corresponds to the active noise (see Appendix A).

Following [29], we find that the steady state solution corresponding to Eq. 8 reads

$$P(x) = N(G(x))^{2(\alpha-1)} \exp \left(\int \frac{2F(y)}{G^2(y)} dy \right), \quad (8)$$

where N is a normalization constant. To derive 8, we assume that the inclusion cannot exit the confining domain and we consider that there is no flux for the inclusion at $x = \pm L$. After identification of the functions F and G from Eq. 7, Eq. 8 becomes

$$P(z) = N e^{-\frac{\eta_c}{\Lambda_c}(V(z)+V_\alpha(z)+U(z))}, \quad (9)$$

where N is a normalization constant and

- (i) $V(z) = \int_0^z f(u) du$ is the confining mechanical potential,
- (ii) $V_\alpha(z) = (1-\alpha)(\Lambda_c/\eta_c) \log(\tilde{L}^2 - z^2)$ corresponds to an effective potential which represents the contribution from the multiplicative noise,
- (iii) $U(z) = (v_0\eta_c/2) \log(\tilde{L}^2 - z^2)$ corresponds to an effective potential which represents the contribution from the boundary flow.

In the following, we show that the interplay of these contributions gives rise to sharp transitions in the shape of the steady state distribution, as displayed in Fig. 2 for $V(z) = kz^2/2$.

To identify the origin of these transitions, it is useful to look at the explicit forms of the distribution in the absence of boundary flow $v_0 = 0$, and confining potential $V(z) = 0$. In the case of thermal fluctuations ($\alpha = 1$) the noise-induced potential vanishes, thus the steady state probability distribution is flat (ie. $P(z) = 1/(2\tilde{L})$), in agreement with the Boltzmann distribution in a flat energy landscape.

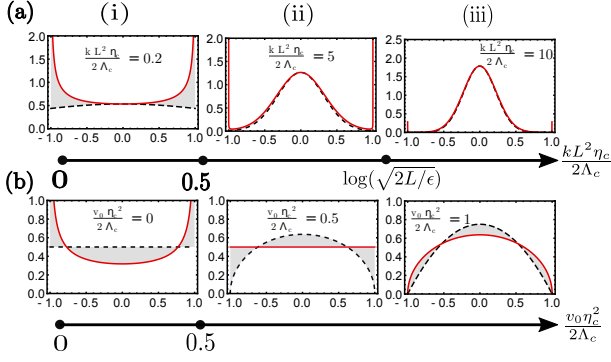


FIG. 2. (color online) Steady-state probability distribution $P(z)$ for the inclusion center of mass (COM) z as a function of (a) the dimensionless stiffness of the confining potential $(kL^2\eta_c)/(2\Lambda_c)$ and (b) of the dimensionless boundary flow $(v_0\eta_c^2)/(2\Lambda_c)$. (a) For an active noise ($\alpha = 1/2$; indicated by a solid red line), we distinguish between three regimes of (i) boundary adhesion, (ii) boundary adhesion with metastable centering and (iii) stable centering. The existence of the boundary adhesion phase in the active situation contrasts with the two phases found in the thermal situation ($\alpha = 1$, dashed black line): a uniform distribution and a stable centering. (b) The active case, $\alpha = 1/2$ (solid red line), shows a transition from (i) boundary adhesion to (iii) stable centering via (ii) a uniform distribution at 0.5.

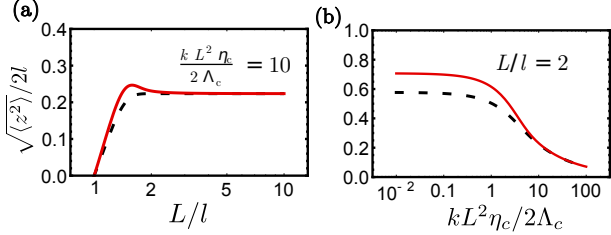


FIG. 3. Variance of the dimensionless COM position $\sqrt{\langle z^2 \rangle}$ for thermal (dashed black line) and active (solid red line) noises, with $v_0 = 0$ as a function of (a) system size L , where it goes from being strongly affected by the boundary, when L is small, to reaching a limiting value determined by the confining strength for large L ; and (b) confining strength $(kL^2\eta_c)/(2\Lambda_c)$, where it asymptotes to a fixed value for small stiffness and goes to zero for large stiffness.

On the other hand, when the noise is active, $\alpha = 1/2$,

$$P(z) = \frac{\pi}{\sqrt{2(\tilde{L}^2 - z^2)}}, \quad (10)$$

Notice that the distribution Eq. 10 diverges at the edges $x = \pm L$; this corresponds to a higher preference of the inclusion to be at the boundaries (see Fig. (2)). The inclusion de-centering occurs although there is no net mechanical force applied to inclusion; this is solely caused due to the noise-induced effective potential V_α .

We point out that, in a more general situation, the divergence can be even stronger than in Eq. 10 and can prevent the distribution from being normalizable. This

situation occurs under the condition that $(v_0\eta_c^2)/(2\Lambda_c) + (\alpha - 1) \leq -1$. Under this condition, depending on the initial condition the inclusion is then fixed at one of the two boundaries at steady state.

We now include the contribution from the confining potential which we assume to be harmonic: $V(z) = kz^2/2$, keeping $v_0 = 0$. We show that the competition between the confining potential – which favors centering the nucleus – and the noise-induced effective potential – which induces adhesion to the cell boundary – leads to a sharp transition as the strength of harmonic potential k or the magnitude of the boundary flow v_0 are varied (Fig. (2)). This can be thought as an active fluctuation-induced wetting-dewetting transition [37].

Since the distribution from Eq. 10 diverges on the two edges, the probability is maximum at the boundary for all values of k . So to compute the phase diagram for harmonic confinement, we regularize it using a cutoff distance ϵ from the boundary, setting its value in this boundary region to be $\int_{L-\epsilon}^L P(z) dz/\epsilon$. The transition point $\log(\sqrt{2L/\epsilon})$ in Fig. (2) is the value of $(kL^2\eta)/(2\Lambda)$ for which this boundary value equals $P(0)$.

Based on Eq. 9, and setting boundary flow $v_0 = 0$, we find that the variance of COM can be expressed in terms of the hypergeometric ${}_1F_1$ and Gamma functions [38],

$$\langle z^2 \rangle = \frac{\tilde{L}^2}{2} \left[\frac{{}_1F_1\left(\frac{3}{2}; (1-\alpha) + \frac{5}{2}; -k\tilde{L}^2\right) \Gamma((1-\alpha) + \frac{3}{2})}{{}_1F_1\left(\frac{1}{2}; (1-\alpha) + \frac{3}{2}; -k\tilde{L}^2\right) \Gamma((1-\alpha) + \frac{5}{2})} \right]. \quad (11)$$

We represent the behavior of Eq. 11 as a function both the system size L of the stiffness of the confining potential k (Fig. (3)). In the limit $k = 0$, the latter expression simplifies into $\langle z^2 \rangle = \tilde{L}^2/2$, when fluctuations are active, and to $\langle z^2 \rangle = \tilde{L}^2/3$ when fluctuations are thermal.

Of course, in a realistic context, one needs to include an *inward pressure* from the compressed active components in the cytoplasm arising from steric hindrance etc., however the symmetry broken de-centering of the steady state distribution due to activity, would still persist.

IV. ELASTIC INCLUSION IN AN ACTIVE FLUID

We next model the inclusion as a passive linear elastic element of unloaded length $2l$, with a stress given by $\sigma^I = B\partial_x u$, where u is the strain from the unloaded configuration and B is the elastic modulus of the inclusion. Similar to Sec. III, the local force balance implies that the bulk stresses are constant, eg. $\sigma^I = \sigma^I(t)$. Hence, integrating σ^I from $z/2 - l$ to $z/2 + l$, we find that the stress along the elastic inclusion reads

$$\sigma^I(t) = \frac{B}{2l} (y - 2l), \quad (12)$$

where $y = \int_{-l}^l \partial_x u$ is the extension of the inclusion. We first derive the general Langevin equation for the inclu-

sion dynamics, before discussing the results for thermal and active fluctuations.

Continuity of stress across the inclusion boundary in the presence of a confining force $f = -\partial_x V$ implies $\sigma^L(t) = \sigma^I(t) + f(x_1)$ and $\sigma^R(t) = \sigma^I(t) - f(x_2)$. After

substitution in Eqs. 5,6, we obtain

$$\eta_c \dot{x}_1 = \eta_c v_L + \frac{B}{2l}(x_1 + L)(y - y_0) - f(x_1)(x_1 + L) - \sqrt{L + x_1} \theta_1, \quad (13)$$

$$\eta_c \dot{x}_2 = -\eta_c v_R + \frac{B}{2l}(x_2 - L)(y - y_0) + f(x_2)(x_2 - L) + \sqrt{L - x_2} \theta_2, \quad (14)$$

where we define the length $y_0 = 2l(1 - \zeta \Delta \mu c_0 / B)$. We perform a change of variable to express Eq. 13 in terms of the vector $\mathbf{X} = [y \ z]^T$, where $y \equiv x_2 - x_1$ is the inclusion length and $z \equiv x_1 + x_2$ is now twice the COM coordinate, to obtain the following multivariate Langevin equation,

$$\dot{\mathbf{X}} = \mathbf{F} + \mathbf{G} \cdot \boldsymbol{\Theta}, \quad (15)$$

where we define the drift vector \mathbf{F} as

$$\mathbf{F} = \frac{1}{\eta_c} \begin{bmatrix} \frac{B}{2l}(y - y_0)(y - 2L) - \eta_c v_0 + f(x_1)(x_1 + L) + f(x_2)(x_2 - L) \\ \frac{B}{2l}(y - y_0)z - f(x_1)(x_1 + L) + f(x_2)(x_2 - L) \end{bmatrix}, \quad (16)$$

and the matrix

$$\mathbf{G} = \sqrt{\frac{2\Lambda_c}{\eta_c^2}} \begin{bmatrix} \sqrt{L + x_1} & \sqrt{L - x_2} \\ -\sqrt{L + x_1} & \sqrt{L - x_2} \end{bmatrix}, \quad (17)$$

which operates on the Gaussian white noise vector $\boldsymbol{\Theta} = [\theta_1 \ \theta_2]^T$. For convenience, we also introduce a diffusion matrix

$$\mathbf{D} = \mathbf{G} \cdot \mathbf{G}^T = \frac{2\Lambda_c}{\eta_c^2} \begin{bmatrix} 2L - y & -z \\ -z & 2L - y \end{bmatrix}. \quad (18)$$

The Fokker-Planck equation corresponding to the Langevin Eq. 15 reads

$$\partial_t P = \frac{\partial}{\partial x_i} \left(-F_i - \alpha \frac{\partial G_{ik}}{\partial x_j} G_{jk} + \frac{1}{2} \frac{\partial}{\partial x_j} G_{ik} G_{jk} \right) P,$$

where we recall that $\alpha = 1$ corresponds to the thermal case and $\alpha = 1/2$ to the active case [35]. Following [29], we introduce the potential vector

$$H_i \equiv \partial_i \log P = D_{ik}^{-1} \left(2F_k + 2\alpha \frac{\partial G_{kl}}{\partial x_j} G_{jl} - \frac{\partial}{\partial x_j} D_{kj} \right),$$

where we consider that repeated latin indices are summed over. Based on Eqs. 16-18, we check that the potential condition

$$\frac{\partial H_i}{\partial x_j} = \frac{\partial H_j}{\partial x_i}, \quad (19)$$

is satisfied. Therefore, the steady state distribution can be expressed as $P(y, z) = N e^{-\Phi}$, where the effective po-

tential Φ reads:

$$\Phi = \frac{\eta_c}{\Lambda_c} \left(\frac{B}{4l}(y - y_0)^2 + V(z + y) + V(z - y) \right) + \left(-\frac{v_0 \eta_c^2}{2\Lambda_c} + (1 - \alpha) \right) \log((2L - y)^2 - z^2). \quad (20)$$

As in the rigid inclusion considered in Sec. III, the effective potential Φ is built from the confining potentials $V(z \pm y)$ (at x_2, x_1 , respectively) and the fluctuation-induced potential $V_\alpha = (1 - \alpha) \log((2L - y)^2 - z^2)$. In addition, the effective potential has a contribution from the elastic energy of the inclusion, $B(y - y_0)^2/(4l)$.

In the case of a harmonic confining potential $V(x_1, x_2) = -k(x_1^2 - x_2^2)$, the potential reads:

$$\Phi = \frac{\eta_c}{\Lambda_c} \left(\left(\frac{B}{4l} + \frac{k}{4} \right) (y - \tilde{y}_0)^2 + \frac{k}{4} z^2 \right) + \left(-\frac{v_0 \eta_c^2}{2\Lambda_c} + (1 - \alpha) \right) \log((2L - y)^2 - z^2), \quad (21)$$

where $\tilde{y}_0 = 2l(B - \zeta \Delta \mu)/(B + kl)$. For $k > -\zeta \Delta \mu c_0$, \tilde{y}_0 is greater than $2l$. We also define the marginal distribution of the inclusion length y as,

$$P(y) \equiv \int_{-(2L-y)}^{2L-y} dz P(y, z), \quad (22)$$

and the marginal distribution of the COM z as

$$P(z) \equiv \int_0^{2L-z} dy P(y, z). \quad (23)$$

With these definitions, we find that, in contrast to the rigid case, the COM distribution for an elastic inclusion

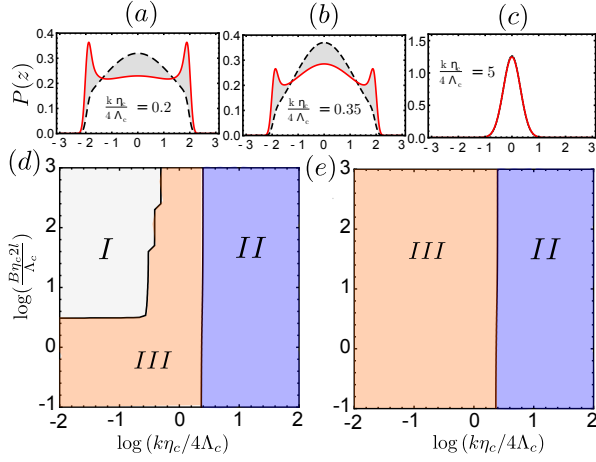


FIG. 4. Marginal distribution of the center of mass (COM, z), and phase plot of most likely COM position, as a function of the dimensionless elasticity of the inclusion ($b = 2LB\eta_c/\Lambda_c$) and the strength of the confinement ($k\eta_c/4\Lambda_c$), for active, and thermal fluctuations and parameter values $2L = 3$, $2l = 1$, and $\zeta\Delta\mu c\eta_c/\Lambda_c = -1$. (a–c) Marginal distribution $P(z)$ of the COM, for active (solid red lines), and thermal (dotted black lines), for $2LB\eta_c/\Lambda_c = 50$ in the de-centered phase I (a), in the boundary phase (b) and in the centered phase II (c). (d) Phase plot showing the most likely COM position for active fluctuations in the (B, k) parameter plane. Different phases correspond to the inclusion being de-centred and extended ($\langle y \rangle > 2l$) (I), centered and compressed ($y < 2l$) (II), and centered and extended (III). Contrast this with the (e) phase plot of the most likely COM position for thermal fluctuations, which has only two phases, where the inclusion is, centered and compressed ($y < 2l$) (II), and centered and extended (III).

cannot be uniform. We define the *centered phase* when the marginal distribution $P(z)$ at the center is highest over the region, else if the probability is maximum off-center, we define as the *de-centered phase*. In the active case $\alpha = 1/2$, the probability $P(z)$ is decentered (resp. centered) for low (resp. high) values of k , as shown in Fig. 4(a)–(c) (solid red curve), contrast this with the thermal case (dotted black curve) where it is centered for all values of k . We find that for active fluctuations, the distribution of the COM position is either peaked on the boundary – de-centered phase (I) – or peaked at the center (centered phase), with inclusion being compressed (II), or extended (III). These transitions in the phase diagram as a function of both the inclusion rigidity B and the confinement strength k are shown in Fig. 4(d). In contrast, as shown in Fig. 4(e), for thermal fluctuations there is only centered phase, with inclusion compressed (II), or extended (III).

In the next two paragraphs, we outline the main differences between thermal and active fluctuations; for simplicity, we first set to zero the boundary flow ($v_0 = 0$), the confining potential ($k = 0$), and the mean activity ($y_0 = 2l$).

In the thermal noise case ($\alpha = 1$), Eq. 20 leads

$$P(y, z) = N \exp \left(-\frac{B}{4lT} (y - y_0)^2 \right), \quad (24)$$

for all $-L + y/2 \leq z \leq L - y/2$, where N is a normalization factor and $\Lambda_c/\eta_c = T$. As expected, Eq. 24 corresponds to a Boltzmann distribution with an elastic energy. The marginal distribution for inclusion length is obtained by integrating Eq. 24 over the coordinate z

$$P(y) = N(2L - y) \exp \left(-\frac{B}{4lT} (y - y_0)^2 \right), \quad (25)$$

which is a Boltzmann distribution although not obvious at first sight. Indeed, the prefactor $(2L - y)$ in Eq. 25 is due to the presence of the confinement, and the no-crossing condition on the inclusion boundary, which limits the z integral range to $2L - y$.

From Eqs. 24, we estimate the moments of the inclusion length and position. For a large normalized elasticity b , the average and variance of the inclusion length converge to $\langle y \rangle = y_0 - (2l)^2/(2L - y_0)b$ and to $\text{Var}[y] = \langle y^2 \rangle - \langle y \rangle^2 = (2l)^2/b$, respectively, while the variance of COM position converges to $\langle x^2 \rangle = ((L - y_0/2)^2/3 + (2l)^2/b)$. These limits match those expected for a rigid inclusion of length y_0 . For small b , the asymptotic value of the averaged and variance of the inclusion length are $\langle y \rangle = 2L/3$ and $\text{Var}[y] = 2L^2/9$, respectively, while the COM variance reads $\langle x^2 \rangle = 2L^2/3$.

In the case of active fluctuations $\alpha = 1/2$, we find that the joint probability distribution reads

$$P(y, z) = \frac{N}{\sqrt{(2L - y)^2 - z^2}} \exp \left(-\frac{B}{4lT} (y - y_0)^2 \right).$$

Integrating over z , we find that the marginal distribution on the inclusion length reads:

$$P(y) = N \exp \left(-\frac{B}{4lT} (y - y_0)^2 \right), \quad (26)$$

where N is a normalization factor. Note that Eq. 26 differs by a prefactor $2L - y$ from the thermal case expression, Eq. 25.

From Eq. 26, we estimate the moments of the inclusion length and position. For a large normalized elastic modulus b , we find that the mean and variance of the inclusion length are, to leading order in $(1/b)$, $\langle y \rangle = y_0$ and $\langle y^2 \rangle - \langle y \rangle^2 = (2l)^2/b$, respectively. Notice that neither the mean nor the variance depends on the confinement length L . To leading order, the variance in the COM position read $\langle x^2 \rangle = ((L - y_0/2)^2/2 + (2l)^2/(2b))$, as expected by comparison with the rigid inclusion case. For small b the asymptotic value of average length is L , variance is $L^2/3$, and the COM variance is $2L^2/3$.

We display the behavior of the moments in the inclusion length and COM position in Fig. 5 (dotted lines for thermal noise, solid lines for active noise). In all cases the value for the thermal fluctuations is smaller than

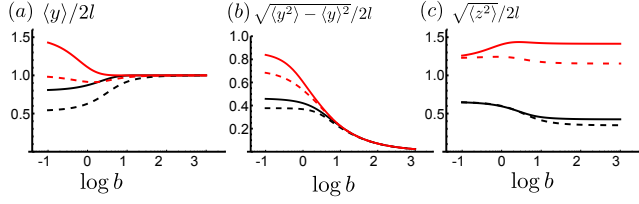


FIG. 5. Moments as a function of the normalized elastic modulus b : (a) mean and (b) standard deviation of the inclusion length y , and (c) variance of the inclusion COM position z . Plotted for two sets of parameters $L/l = 1.6$ (black curve), and $L/l = 3$ (red curve), where we have fixed $y_0 = 2l = 1$, for both thermal fluctuation (dotted line), and active fluctuation (solid line). Thermal fluctuations exhibit reduced moments compared to the active, for both sets of parameters. For large b , we recover the rigid inclusion moments (see Sec. III), while for small b the moments converge to the calculated asymptotic limit (see Sec. IV).

that for active fluctuations of same strength. The differences in the mean and variance of the inclusion length is quite significant for small values of b and decreases with increase in b ; contrast this with the variance of COM for which the differences grow with increasing value of b . Note that unlike in Fig. 4(a), the variation of $\langle y \rangle$ in Fig. 5(a) is a fluctuation effect. For $L/l < 2$ we observe a rather surprising behaviour - the mean length of the inclusion for large fluctuation (small stiffness) is less than for small fluctuations (large stiffness) - as opposed to the case when $L/l > 2$ where the average length increases with increase in fluctuation. This behaviour can be understood in terms of the asymptotic values mentioned, for large b its the free length $2l$, for small b its governed by the confinement size, and is equal to L .

where the drift force is

$$\mathbf{F} = \frac{1}{\gamma(y)} \left[\begin{array}{c} -(2L - y)\frac{B}{2l}(y - y_0) - \eta_c v_0 + f(x_1)(L + x_1) + f(x_2)(x_2 - L) \\ z \left(\frac{B}{2l}(y - y_0) - \frac{\eta_I}{2l} v_0 \right) + \frac{(\gamma(y) + \frac{\eta_I}{2l} z)f(x_2)(x_2 - L)}{\eta_c} + \frac{(-\gamma(y) + \frac{\eta_I}{2l} z)f(x_1)(L + x_1)}{\eta_c} \end{array} \right],$$

the noise amplitude matrix is

$$\mathbf{G} = \left[\begin{array}{cc} \frac{\sqrt{2\Lambda_c(L + x_1)}/\gamma(y)}{(-1 + \frac{\eta_I z}{2l\gamma(y)})\sqrt{2\Lambda_c(L + x_1)}/\eta} & \frac{\sqrt{2\Lambda_c(L - x_2)}/\gamma(y)}{(1 + \frac{\eta_I z}{2l\gamma(y)})\sqrt{2\Lambda_c(L - x_2)}/\eta} \end{array} \right],$$

$\Theta = [\theta_1 \ \theta_2]^T$ is Gaussian white noise of unit variance; $\gamma(y) \equiv \eta_c + \eta_I(2L - y)/(2l)$ is a friction that depends on the inclusion length y , and $y_0 \equiv 2l(1 - (\zeta\Delta\mu c_0)/B)$ is the activity-renormalized rest length.

For a general confining force, the Fokker-Planck equation associated with Eq. 28 does not satisfy the potential condition (Eq. 19), which implies the existence of a non-zero probability current J_i , even at steady state. This can be seen from the fact that keeping the dissipation

V. KELVIN-VOIGT INCLUSION

Lastly, we consider the case when the inclusion is viscoelastic of a Kelvin-Voigt type (i.e., it behaves elastically at the longest time scales). This situation is closer to a realistic description of the cell nucleus embedded in the active cytoplasm, since, as reported in [7, 28, 39], the noise on the nucleus is dominated by active cytoskeletal processes. As in the previous section, the unloaded length of the inclusion is denoted $2l$, the displacement from the unloaded configuration is u and the elastic modulus is B ; thus the elastic stress is equal to $B\partial_x u$. In addition, we include the dissipative contribution ($\eta_I\partial_x \dot{u}$) into the stress equation

$$\sigma^I = B\partial_x u + \eta_I\partial_x \dot{u}, \quad (27)$$

where η_I is the internal viscosity of the inclusion. Following the analysis in the previous sections, force balance within the inclusion implies that $\sigma^I = \sigma^I(t)$; integrating Eq. 27 over the reference length $x - l$ to $x + l$ leads to the relation,

$$2l\sigma^I(t) = B(y - 2l) + \eta_I \dot{y}.$$

From the force balance condition on the two inclusion edges, we obtain the following multivariate Langevin equation on the variables $\mathbf{X} = [y \ z]^T$:

$$\dot{\mathbf{X}} = \mathbf{F} + \mathbf{G} \cdot \Theta, \quad (28)$$

term in the inclusion without the corresponding fluctuation source, violates FDT, and makes it essentially a two-temperature problem, with inclusion temperature set to zero.

To analyze the dynamics when fluctuations are thermal, i.e., when both the inclusion and the surrounding fluid are at equal temperature T , we set $\Lambda_c = \eta_c k_B T$, and inclusion stress is given by,

$$\sigma^I = B\partial_x u + \eta_I\partial_x \dot{u} + \sqrt{2\eta_I k_B T} \theta, \quad (29)$$

where θ is unit variance Gaussian white noise. The steady state probability distribution obtained using the inclusion stress in Eq. 29, is exactly the same as that obtained for the elastic inclusion with thermal fluctuation (Eq. 24) in Section IV.

In the absence of any kind of external potential in Eq. 28, the potential condition is satisfied, and the steady state is $P(y, z) = Ne^{-\Phi}$, with

$$\begin{aligned} \Phi = & \frac{b}{r} \left(\frac{y}{2l} \left(\frac{\alpha}{b} - d - 1 \right) + \frac{1}{2} \left(\frac{y}{2l} \right)^2 (d + r + 1) - \frac{1}{3} \left(\frac{y}{2l} \right)^3 \right) \\ & + \left((1 - \alpha) - \frac{\eta_c^2 v_0}{2\Lambda_c} \right) \log((2L - y)^2 - z^2) \\ & + 2(\alpha - 1) \log \gamma(y), \end{aligned} \quad (30)$$

where $b = (2LB\eta_c)/\Lambda_c$ is the ratio of two stresses, the inclusion elastic stress $2LB$ and the fluctuating stress Λ_c/η_c , $r = \eta_c/\eta_I$, the ratio of the two viscosities, and $d = L/l$ the ratio of size of confinement to the inclusion.

Note that in the limit $\alpha = 1$, the effective potential Φ is cubic, and not harmonic. This is because, as discussed above, for $\alpha = 1$ this does not reduce to an isothermal description. It corresponds to a two-temperature problem, where the inclusion is connected to a bath at temperature zero, and surrounding fluid to a bath at temperature $\Lambda_c/k_B\eta_c$. This makes it inherently non-equilibrium, with an equilibrium description, in terms of an effective potential which has a very different form the actual potential of the system.

In the following, we focus on the effect of active fluctuations, for which we take $\alpha = 1/2$, while we fix the other parameters at $v_0 = 0$, $\zeta = 0$, $d = L/l = 4$ and $y_0 = 2l = 1$.

Fig. 6(a) shows a contour plot of the average inclusion length as function of stress ratio b , and viscosity ratio r . In Fig. 6(b), we take a cut across the contour plot, to show the average length as a function of viscosity ratio for two different values of b , the stress ratio. We find that for softer inclusions ($b = 0.1$), the effective inclusion size is negligibly small when the inclusion viscosity is large (compared to the cytoplasm), and increases to beyond its unloaded length $2l$ when the inclusion viscosity is small. On the other hand for stiffer inclusions ($b = 10$), the effective inclusion size is larger than $2l$ when the inclusion viscosity is large, and shrinks to below $2l$ when the inclusion viscosity is small. Similarly, Fig. 6(c) is plotted with respect to the stress ratio b . Unexpectedly, the inclusion shrinks either when the inclusion stiffness is increased or when the viscosity is decreased.

We display in Figs. 7 and 8 how the amplitude of fluctuations - of both the width and COM position - vary as a function of b and r . As expected, a stiffer inclusion generally correspond to a lower amplitude in the fluctuations of the width; less intuitive is the observation that a stiffer inclusion leads to an increase of fluctuations in COM.

VI. FORCE ON THE CONFINING WALLS SITUATED AT THE CELL BOUNDARY

We now determine the force induced by the fluctuating inclusion at the confining walls situated at the cell

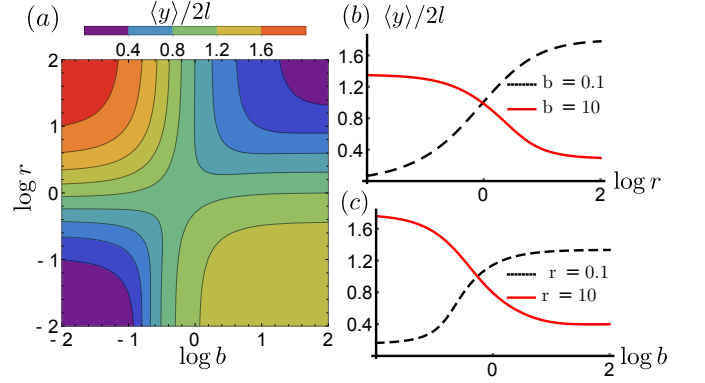


FIG. 6. (a) Contour plot of the mean inclusion size $\langle y \rangle$ as function of the stress ratio b and the viscosity ratio r , keeping the other parameters fixed (see text). (b,c) Mean inclusion size $\langle y \rangle$ versus r and b , respectively.

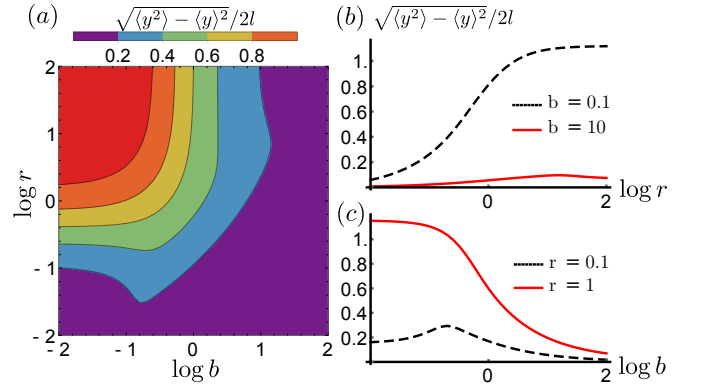


FIG. 7. (a) Contour plot of the standard deviation of inclusion size $\sqrt{\langle y^2 \rangle - \langle y \rangle^2}$ as function of the stress ratio b and the viscosity ratio r , all other parameters fixed. (b,c) Standard deviation of inclusion size y versus r and b , respectively.

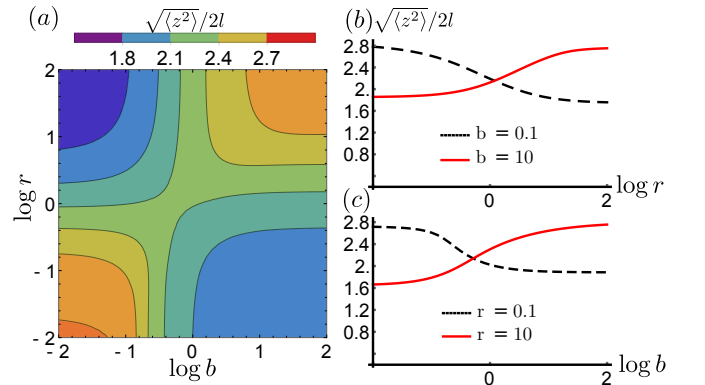


FIG. 8. (a) Contour plot of the standard deviation of centre of mass position of the inclusion $\sqrt{\langle z^2 \rangle}$ as function of the stress ratio b and the viscosity ratio r , all other parameters fixed. (b,c) Mean centre of mass position $\sqrt{\langle z^2 \rangle}$ versus r and b , respectively.

boundary. This force depends on the specific nature of the fluctuations, and is a non-equilibrium Casimir force [40–42].

Not surprisingly, the form of the force depends on the physical nature of the inclusion. In the case of a rigid inclusion and in the absence of a confining potential, the local stress at the boundary reads $\sigma = -\zeta\Delta\mu c_0 + (\sqrt{2\tilde{L}\theta})/(2\tilde{L})$, whose mean is $\langle\sigma\rangle = -\zeta\Delta\mu c_0$. There is no fluctuation contribution to the average boundary force, irrespective of whether the noise is thermal [43] or active.

In the elastic inclusion case, the average stress on the confining walls is given by $\langle\sigma\rangle = B(\langle y\rangle - 2l)/(2l)$. As discussed in Section IV, the average inclusion size $\langle y\rangle$ depends on the strength and nature of the noise (whether thermal or active).

In Fig. 9(a) we assume a fixed stiffness; we represent the average stress as a function of the inverse amplitude of fluctuation. When the amplitude of fluctuation Λ_c/η_c is weak compared to the elastic stress (large b), the fluctuation contribution to the force on the walls converges to zero – this corresponds to the rigid inclusion result. For large fluctuations, the sign of the force depends on L/l , the ratio of size of confinement to size of inclusion. For comparable size (black curve) it is attractive, and for an inclusion much smaller than confinement scale (red curve), it is repulsive (positive value of stress).

The average stress is a decreasing function of the elastic modulus B when the confinement size is large compared to the inclusion width (as seen in Fig. 9(b), red curves). However, the average stress can become an increasing function of B for larger inclusion width. As expected from the rigid inclusion case, the force on the walls vanishes when the elastic strength $2lB$ becomes small compared to the fluctuation strength Λ_c/η_c . For large stiffness B , the asymptotic value of the averaged stress depends on whether the noise is thermal or active: for thermal noise, the averaged stress becomes attractive, with an amplitude that is controlled by the ratio L/l ; for active noise, the averaged stress vanishes. The presence of an effective force between the walls, even for thermal fluctuations, shows that inhomogeneity in form of inclusions has nontrivial implications.

VII. CONCLUSION

Starting from 1D fluctuating active hydrodynamics we derive a Langevin dynamics description of an embedded inclusion. We find that the stochastic dynamics of the inclusion centre of mass and length is given by coupled Langevin equations with multiplicative noise.

We analyze three different inclusion types, rigid, elastic, and viscoelastic (Kelvin-Voigt). For all these cases we can analytically obtain the steady state probability distribution.

In the simplest description of the inclusion as a

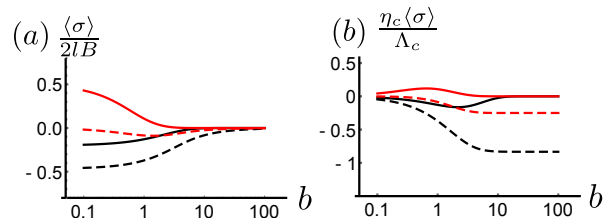


FIG. 9. Average stress for an elastic inclusion embedded in a viscous fluid subject to thermal (dotted line) and active (solid line) noise, for $2l = 1$, $2L = 2$ (black), and $2L = 3$ (red) as function of b , the ratio of the elastic to the fluctuating stress. In (a) the stress is expressed in units of the elastic stress $\langle\sigma\rangle/2lB$ and plotted as a function of η_c/Λ_c , for fixed B , while in (b) the stress is in units of the fluctuation stress $\langle\sigma\rangle\eta_c/\Lambda_c$ and plotted as a function of B , for fixed η_c/Λ_c .

rigid object, we obtain analytical expression for the steady state distribution, which reveal the existence of a fluctuation-induced effective potential. This attractive force, which originates from the non-equilibrium nature the noise, is reminiscent of Casimir forces in non-equilibrium systems [40–42].

Considering the inclusion as an elastic element introduces an additional degree of freedom along with centre of mass, namely the extension or the inclusion length. The effective attraction between the inclusion and the confining walls persists, with the noise induced force dependent on the length of the inclusion. We find that the average length of the elastic inclusion depends non-trivially on the size of confinement and strength of the fluctuation.

Unlike the rigid and elastic description, a Kelvin-Voigt viscoelastic description of the inclusion, in general cannot be mapped to an equilibrium system with an effective potentials. Nevertheless, it is possible to have an effective equilibrium description in the absence of external confining forces. We find that the viscosity of the inclusion is a crucial parameter, the mean and variances of the inclusion length strongly depend on the viscosity ratio of the inclusion and the outside fluid, along with its stiffness and stress fluctuation.

Since the observed phenomena are due to the multiplicative and active nature of the noise, we believe these noise induced interactions should occur in a variety of biological and in-vitro contexts. We list a few here: (i) the positioning and shape fluctuations of the nucleus (or other localized organelles) within a cell, (ii) the dynamics of large colloidal particles embedded in an active medium, (iii) the positioning and dynamics of nuclei in multi-nucleated cells, (iv) the positioning and segregation of chromosomes within a nucleus and (v) the fluctuations of a cell within a developing tissue. Our study of the active Casimir-like forces at the cell boundary, arising from nuclear stiffness and fluctuations might be relevant to rigidity sensing by focal adhesions [44].

We are currently extending our study to the case when the (nuclear) inclusion is subject to its own source of ac-

tive fluctuation, in addition to the noise coming from the surrounding active fluid. We are also studying the collective dynamics of colloids [45, 46] embedded in an active fluid in higher dimensions, where the hydrodynamic interactions lead to multiplicative noise.

VIII. ACKNOWLEDGEMENT

We thank S. Ramaswamy, F. Julicher, K. Vijaykumar, and R. Morris for clarifying discussions, as well as A. Rautu and K. Husain for help in the manuscript. AS thanks MBI-Singapore and J.-F.R. thanks NCBS-Bangalore for hospitality.

Appendix A: Overdamped Langevin equation from generalised Langevin dynamics

In general overdamped Langevin equations with multiplicative delta-function noise are ill defined - they result in different Fokker-Planck descriptions under different choices of stochastic calculus used to discretize the noise term [30, 35]. Hence, overdamped Langevin equations with multiplicative delta-function noise, must be provided with an interpretation of the noise, in order to be meaningful.

An unambiguous approach is to start with the correct microscopic inertial dynamics for all the microscopic variables, and establish a separation of time scales. One then systematically integrates over the shorter time scales to arrive at the correct overdamped Langevin equations. We start with a generalized underdamped Langevin dynamics for a particle position $x(t)$, with spatially varying damping and a noise θ that satisfies an Ornstein-Uhlenbeck process [29],

$$\begin{aligned} \dot{x} &= v, \\ m\dot{v} + \gamma(x)v &= f(x) + g(x)\frac{\theta}{\sqrt{\tau_n}}, \\ \dot{\theta} &= -\frac{1}{\tau_n}\theta + \frac{1}{\sqrt{\tau_n}}\vartheta, \end{aligned} \quad (\text{A1})$$

where $\langle \vartheta(t)\vartheta(t') \rangle = 2\Lambda\delta(t-t')$. The other relevant time scale is the inertial relaxation time $\tau_m = \gamma(x)/m$.

To go from here to an overdamped Langevin equation with white noise, it is necessary to take the two limits : $\tau_m \rightarrow 0$ to get the overdamped dynamics, and $\tau_n \rightarrow 0$, to get the white-noise limit. However, as discussed in [31], one might choose to take these limits in different order, which result in different interpretations of the overdamped equations. Since Langevin dynamics corresponding to thermal noise is constrained to obey the fluctuation-dissipation relation (FDR), it is convenient to treat the thermal and active noise cases separately.

1. Thermal

A necessary condition for the Langevin dynamics Eq. A1 to describe thermal noise is that $\tau_n \rightarrow 0$, which leads to

$$\begin{aligned} m\dot{v} + \gamma(x)v &= f(x) + g(x)\vartheta, \\ \dot{x} &= v. \end{aligned} \quad (\text{A2})$$

The corresponding Fokker-Planck is,

$$\partial_t P = -\partial_x v P + \frac{1}{m} \partial_v \left(\gamma(x)v - f(x) + \frac{\Lambda}{m} g^2(x) \partial_v \right) P \quad (\text{A3})$$

To obtain the overdamped Langevin equation from the Fokker-Planck equation A3, we use the technique of adiabatic elimination in the momentum variable [29, 47, 48].

Define the moments of v , $Q_k = \int dv v^k P$. The equations for the moments of v are,

$$\begin{aligned} \frac{\partial}{\partial t} Q_0 &= -\frac{\partial}{\partial x} Q_1 \\ \frac{\partial}{\partial t} Q_1 &= -\frac{\partial}{\partial x} Q_2 - \frac{\gamma(x)}{m} Q_1 + \frac{f(x)}{m} Q_0 \\ \frac{\partial}{\partial t} Q_2 &= -\frac{\partial}{\partial x} Q_3 - \frac{2\gamma(x)}{m} Q_2 + \frac{2f(x)}{m} Q_1 + 2\Lambda \frac{g^2(x)}{m^2} Q_0 \end{aligned}$$

and so on. Thus to solve for Q_0 , we require knowledge of higher moments. However, we note that the k^{th} -moments decay exponentially fast with a time scale proportional to τ_m . Thus in the limit $\tau_m \rightarrow 0$, we can assume the higher moments reach steady state, from which we obtain,

$$Q_2 = -\frac{m}{2\gamma(x)} \frac{\partial}{\partial x} Q_3 + \frac{f(x)}{\gamma(x)} Q_1 + \Lambda \frac{g^2(x)}{m\gamma(x)} Q_0 \quad (\text{A4})$$

$$Q_1 = -\frac{m}{\gamma(x)} \frac{\partial}{\partial x} Q_2 + \frac{f(x)}{\gamma(x)} Q_0 \quad (\text{A5})$$

Using these relation in the equation for Q_0 , and ignoring terms of order τ_m and higher, we obtain,

$$\frac{\partial}{\partial t} Q_0 = \frac{\partial}{\partial x} \left(-\frac{f(x)}{\gamma(x)} Q_0 + \frac{\Lambda}{\gamma(x)} \frac{\partial}{\partial x} \left(\frac{g^2(x)}{\gamma(x)} Q_0 \right) \right).$$

If the fluctuations are thermal then FDR holds, and $\gamma(x) = g^2(x)$, and $\Lambda = k_B T$, where T is temperature of the bath, and the above equation reduces to,

$$\partial_t Q_0 = \partial_x \left(-\frac{f(x)}{\gamma(x)} + \frac{k_B T}{\gamma(x)} \frac{\partial}{\partial x} \right) Q_0. \quad (\text{A6})$$

The corresponding Langevin equation

$$\gamma(x)\dot{x} = f(x) + g(x)\vartheta, \quad (\text{A7})$$

is interpreted in Hanggi-Klimontovich convention [33, 34].

2. Active

On the other hand, by not setting τ_n to zero, we are necessarily describing a situation where the noise is athermal. This is consistent with an active noise, where the microscopic variables (actomyosin remodeling and turnover) describing active noise are slower than the inertial relaxation time, $\tau_m \ll \tau_n$.

Taking $\tau_m \rightarrow 0$ in A1, we get,

$$\begin{aligned} v &= \frac{f(x)}{\gamma(x)} + \frac{g(x)}{\gamma(x)} \frac{\theta}{\sqrt{\tau_n}} \\ \dot{\theta} &= -\frac{1}{\tau_n} \theta + \frac{1}{\sqrt{\tau_n}} \vartheta \end{aligned} \quad (\text{A8})$$

The corresponding Fokker-Planck is,

$$\begin{aligned} \frac{\partial}{\partial t} P &= -\frac{\partial}{\partial x} \left(\frac{f(x)}{\gamma(x)} + \frac{1}{\sqrt{\tau_n}} \frac{g(x)}{\gamma(x)} \theta \right) P \\ &\quad + \frac{1}{\tau_n} \frac{\partial}{\partial \theta} \left(\theta + \Lambda \frac{\partial}{\partial \theta} \right) P \end{aligned} \quad (\text{A9})$$

We define the moment of θ , $Q_k = \int d\theta \theta^k P$. From A9 we obtain,

$$\begin{aligned} \frac{\partial}{\partial t} Q_0 &= -\frac{\partial}{\partial x} \frac{f(x)}{\gamma(x)} Q_0 - \frac{1}{\sqrt{\tau_n}} \frac{\partial}{\partial x} \frac{g(x)}{\gamma(x)} Q_1 \\ \frac{\partial}{\partial t} Q_1 &= -\frac{\partial}{\partial x} \frac{f(x)}{\gamma(x)} Q_1 - \frac{1}{\sqrt{\tau_n}} \frac{\partial}{\partial x} \frac{g(x)}{\gamma(x)} Q_2 - \frac{1}{\tau_n} Q_1 \\ \frac{\partial}{\partial t} Q_2 &= -\frac{\partial}{\partial x} \frac{f(x)}{\gamma(x)} Q_2 - \frac{1}{\sqrt{\tau_n}} \frac{\partial}{\partial x} \frac{g(x)}{\gamma(x)} Q_3 - \frac{2}{\tau_n} Q_2 + \frac{2\Lambda}{\tau_n} Q_0 \end{aligned}$$

and so on. Following the arguments in the case of thermal

noise, we obtain, in the limit $\tau_n \rightarrow 0$,

$$Q_1 = -\sqrt{\tau_n} \frac{\partial}{\partial x} \frac{g(x)}{\gamma(x)} Q_2 - \tau_n \frac{\partial}{\partial x} \frac{f(x)}{\gamma(x)} Q_1 \quad (\text{A10})$$

$$Q_2 = -\frac{\sqrt{\tau_n}}{2} \frac{\partial}{\partial x} \frac{g(x)}{\gamma(x)} Q_3 - \frac{\tau_n}{2} \frac{\partial}{\partial x} \frac{f(x)}{\gamma(x)} Q_2 + \Lambda Q_0 \quad (\text{A11})$$

which leads to

$$\frac{\partial}{\partial t} Q_0 = -\frac{\partial}{\partial x} \frac{f(x)}{\gamma(x)} Q_0 + \Lambda \frac{\partial}{\partial x} \frac{g(x)}{\gamma(x)} \frac{\partial}{\partial x} \frac{g(x)}{\gamma(x)} Q_0 \quad (\text{A12})$$

The corresponding Langevin equation

$$\gamma(x) \dot{x} = f(x) + g(x) \vartheta, \quad (\text{A13})$$

is interpreted in the Stratonovich convention[29, 32].

Appendix B: Constant total myosin number

If the myosin turnover is slow compared to the time scales of interest, the total number of myosin in the two segments L(R) can be taken to be constant $c_{L(R)}$. With this, we obtain from Eqs. 3, 4,

$$\begin{aligned} \eta_c \dot{x}_1 &= \eta_c v_L + (x_1 + L) \sigma^L(t) + \zeta \Delta \mu c_L - \int_{-L}^{x_1} \vartheta dx \\ \eta_c \dot{x}_2 &= -\eta_c v_R + (x_2 - L) \sigma^R(t) - \zeta \Delta \mu c_R + \int_{x_2}^L \vartheta dx \end{aligned}$$

Comparing this with Eqns. 5, 6 we see that, the effect of the constant myosin number is same as having a boundary flow $v_0 = \zeta \Delta \mu c_L / \eta_c$. In this paper, we have treated the mean contractile stress $\zeta \Delta \mu$ and noise amplitude Λ as independent. In reality, they have a common origin in the actomyosin remodeling dynamics, and Λ depends on $\zeta \Delta \mu$ [27].

If $\Lambda = \Lambda_0 c$, the actomyosin density, and we assume slow turnover of actomyosin, then the noise θ will be additive.

The equations then reduce to,

$$\begin{aligned} \eta_c \dot{x}_1 &= \eta_c v_L + (x_1 + L) \sigma^L(t) + \zeta \Delta \mu c_L - \sqrt{2\Lambda_0 c_L} \theta_1 \\ \eta_c \dot{x}_2 &= -\eta_c v_R + (x_2 - L) \sigma^R(t) - \zeta \Delta \mu c_R + \sqrt{2\Lambda_0 c_R} \theta_2 \end{aligned}$$

where $\theta_{1(2)}$ are unit variance Gaussian white noises.

-
- [1] M. C. Marchetti, J. F. Joanny, S. Ramaswamy, T. B. Liverpool, J. Prost, M. Rao, and R. A. Simha, *Reviews of Modern Physics* **85**, 1143 (2013).
 - [2] J. Prost, F. Jülicher, and J.-F. Joanny, *Nature Physics* **11**, 111 (2015).
 - [3] A. P. Solon, Y. Fily, A. Baskaran, M. E. Cates, Y. Kafri, M. Kardar, and J. Tailleur, *Nature Physics* **11**, 1 (2015), arXiv:1412.3952v2.
 - [4] I. Dupin and S. Etienne-Manneville, *International Journal of Biochemistry and Cell Biology* **43**, 1698 (2011).
 - [5] G. G. Gundersen and H. J. Worman, *Cell* **152**, 1376 (2013).
 - [6] N. R. Morris, *Current Opinion in Cell Biology* **15**, 54 (2002).
 - [7] E. Makhija, D. S. Jokhun, and G. V. Shivashankar, *Proceedings of the National Academy of Sciences* **113**, E32 (2016).
 - [8] S. Talwar, A. Kumar, M. Rao, G. I. Menon, and G. Shivashankar, *Biophysical Journal* **104**, 553 (2013).
 - [9] D. Weihs, T. G. Mason, and M. A. Teitell, *Biophysical*

- Journal **91**, 4296 (2006).
- [10] F. M. Hameed, M. Rao, and G. V. Shivashankar, *PloS one* **7**, e45843 (2012).
 - [11] A. Lau, B. Hoffman, A. Davies, J. Crocker, and T. Lubensky, *Physical Review Letters* **91**, 7 (2003).
 - [12] É. Fodor, M. Guo, N. S. Gov, P. Visco, D. a. Weitz, and F. van Wijland, *EPL (Europhysics Letters)* **110**, 48005 (2015), arXiv:arXiv:1505.06489v1.
 - [13] A. Mazumdar and M. Mazumdar, *BioEssays* **24**, 1012 (2002).
 - [14] T. Cremer and C. Cremer, *Nature reviews. Genetics* **2**, 292 (2001).
 - [15] R. Bruinsma, A. Y. Grosberg, Y. Rabin, and A. Zidovska, *Biophysical journal* **106**, 1871 (2014).
 - [16] S. C. Weber, A. J. Spakowitz, and J. A. Theriot, *Proceedings of the National Academy of Sciences of the United States of America* **109**, 7338 (2012).
 - [17] N. Ganai, S. Sengupta, and G. I. Menon, *Nucleic acids research*, 1 (2014).
 - [18] D. L. Barton, S. Henkes, C. J. Weijer, and R. Sknepnek, 1 (2016), arXiv:1612.05960v1.
 - [19] S. Curran, C. Strandkvist, J. Bathmann, M. de Gennes, A. Kabla, G. Salbreux, and B. Baum, *bioRxiv* (2016), 10.1101/078204.
 - [20] Q. Li, A. Kumar, E. Makhija, and G. Shivashankar, *Biomaterials* **35**, 961 (2014).
 - [21] J. F. Rupprecht, A. Singh, G. V. Shivshankar, M. Rao, and J. Prost, (2017), arXiv:1703.04395.
 - [22] D. Bartolo, A. Ajdari, and J.-B. Fournier, *Physical review. E, Statistical, nonlinear, and soft matter physics* **67**, 061112 (2003), arXiv:0304356 [cond-mat].
 - [23] D. Ray, C. Reichhardt, and C. J. O. Reichhardt, *Physical Review E - Statistical, Nonlinear, and Soft Matter Physics* **90**, 1 (2014), arXiv:arXiv:1402.6372v1.
 - [24] C. Parra-Rojas and R. Soto, *Physical Review E - Statistical, Nonlinear, and Soft Matter Physics* **90**, 1 (2014), arXiv:1404.4857.
 - [25] A. Saha, M. Nishikawa, M. Behrndt, C.-P. Heisenberg, F. Jülicher, and S. W. Grill, *Biophysical Journal* **110**, 1421 (2016), arXiv:1507.00511.
 - [26] K. Kruse, J. F. Joanny, F. Jülicher, J. Prost, and K. Sekimoto, *European Physical Journal E* **16**, 5 (2005), arXiv:0406058 [physics].
 - [27] A. Basu, J. F. Joanny, F. Jülicher, and J. Prost, *The European physical journal. E, Soft matter* **27**, 149 (2008).
 - [28] M. Versaevel, T. Grevesse, and S. Gabriele, *Nature communications* **3**, 671 (2012).
 - [29] C. W. Gardiner, *Stochastic Methods: A Handbook for the Natural and Social Sciences*, 4th ed. (Springer, 2009).
 - [30] N. G. van Kampen, *Journal of Statistical Physics* **24**, 175 (1981).
 - [31] R. Kupferman, G. A. Pavliotis, and A. M. Stuart, *Physical Review E - Statistical, Nonlinear, and Soft Matter Physics* **70**, 036120 (2004).
 - [32] R. Stratonovich, *SIAM Journal on Control* **4**, 362 (1966).
 - [33] P. Hänggi and H. Thomas, *Physics Reports* **88**, 207 (1982).
 - [34] Y. Klimontovich, *Physica A: Statistical Mechanics and its Applications* **163**, 515 (1990).
 - [35] A. W. C. Lau and T. C. Lubensky, *Physical Review E* **76** (2007), 10.1103/PhysRevE.76.011123, arXiv:0707.2234.
 - [36] T. Kuroiwa and K. Miyazaki, *Journal of Physics A: Mathematical and Theoretical* **47**, 012001 (2014), arXiv:1309.4189.
 - [37] P. G. de Gennes, *Reviews of Modern Physics* **57**, 827 (1985).
 - [38] G. Arfken, Weber, and Harris, *Mathematical Methods for Physicists*, 7th ed. (Elsevier, Orlando FL, 2012).
 - [39] N. M. Ramdas and G. V. Shivashankar, *Journal of Molecular Biology* **427**, 695 (2015).
 - [40] A. Aminov, Y. Kafri, and M. Kardar, *Physical Review Letters* **114**, 230602 (2015), arXiv:1501.01006.
 - [41] R. Brito, U. Marini Bettolo Marconi, and R. Soto, *Physical Review E - Statistical, Nonlinear, and Soft Matter Physics* **76**, 1 (2007), arXiv:0611233 [cond-mat].
 - [42] T. R. Kirkpatrick, J. M. Ortiz De Zarate, and J. V. Sengers, *Physical Review Letters* **110**, 1 (2013), arXiv:arXiv:1302.4704v1.
 - [43] C. Monahan, A. Naji, R. Horgan, B.-S. Lu, and R. Podgornik, *Soft Matter* (2015), 10.1039/C5SM02346G, arXiv:arXiv:1310.1965v3.
 - [44] X. Cao, Y. Lin, T. P. Driscoll, J. Franco-Barraza, E. Cukierman, R. L. Mauck, and V. B. Shenoy, *Biophysical Journal* **109**, 1807 (2015).
 - [45] J. Happel and H. Brenner, *Low Reynolds number hydrodynamics*, Mechanics of fluid and transport processes, Vol. 1 (Springer, Netherlands, 1983).
 - [46] M. Doi and S. F. Edwards, *The Theory of Polymer Dynamics* (Oxford University Press, 1988).
 - [47] R. Fox, *Physical Review A* **33**, 467 (1986).
 - [48] A. Baule, K. V. Kumar, and S. Ramaswamy, *Journal of Statistical Mechanics: Theory and Experiment* **11008**, 11 (2009), arXiv:0903.1572.